Musculoskeletal simulations to examine the effects of accentuated eccentric loading (AEL) on jump height

Eric Yung-Sheng Su [Corresp., 1], **Timothy J Carroll** [1], **Dominic J Farris** [1, 2], **Glen A Lichtwark** [1]

[1] Faculty of Health and Behavioural Sciences, University of Queensland, Brisbane, Queensland, Australia

[2] Sport and Health Sciences, College of Life and Environmental Sciences, University of Exeter, Exeter, Devon, United Kingdom

Corresponding Author: Eric Yung-Sheng Su
Email address: yungsheng.su@uq.edu.au

Background

During counter movement jumps, adding weight in the eccentric phase and then suddenly releasing this weight during the concentric phase, known as accentuated eccentric loading (AEL), has been suggested to immediately improve jumping performance. The level of evidence for the positive effects of AEL remains weak, with conflicting evidence over the effectiveness in enhancing performance. Therefore, we proposed to theoretically explore the influence of implementing AEL during constrained vertical jumping using computer modelling and simulation and examined whether the proposed mechanism of enhanced power, increased elastic energy storage and return, could enhance work and power.

Methods

We simulated human jumping motion with a simplified model, consisting of a ball-shaped body (head, arm, and trunk), two lower limb segments (thigh and shank), and four muscles. We adjusted the key activation parameters of the muscles to influence the performance outcome of the model. Numerical optimization was applied to search the optimal solution for the model. We implemented AEL and non-AEL conditions in the model to compare the simulated data between conditions.

Results

Our model predicted that the optimal jumping performance was achieved when the model utilized the whole joint range. However, there was no difference in jumping performance in AEL and non-AEL conditions because the model began its push-off at the similar state (posture, fiber length, fiber velocity, fiber force, tendon length, and the same activation level). Therefore, the optimal solution predicted by the model was primarily driven by intrinsic muscle dynamics (force-length-velocity relationship), and this coupled with the similar model state at the start of the push-off, resulting in similar push-off performance across all conditions. There was also no evidence of additional tendon-loading effect in AEL conditions compared to non-AEL condition.

Discussion

Our simulation results disagree with some experimental studies that reported increased jump performance with AEL. We suspect that, in some experimental studies, AEL's performance-enhancing effect might be caused by differences in activation strategies between those undertaken by humans and those found through our model optimization, or due to the simplicity of our model.

Musculoskeletal simulations to examine the effects of accentuated eccentric loading (AEL) on jump height.

Eric Yung-Sheng Su[1], Timothy John Carroll[1], Dominic James Farris[1,2], Glen Anthony Lichtwark[1]

[1] School of Human Movement and Nutrition Sciences, The University of Queensland, Brisbane, Queensland, Australia

[2] Sport and Health Sciences, College of Life and Environmental Sciences, University of Exeter, Exeter, Devon, United Kingdom

Corresponding Author:

Eric Su[1]

Human Movement Studies Building, St Lucia, Brisbane, Queensland, 4067, Australia

Email address: yungsheng.su@uq.edu.au

Abstract

Background

During counter movement jumps, adding weight in the eccentric phase and then suddenly releasing this weight during the concentric phase, known as accentuated eccentric loading (AEL), has been suggested to immediately improve jumping performance. The level of evidence for the positive effects of AEL remains weak, with conflicting evidence over the effectiveness in enhancing performance. Therefore, we proposed to theoretically explore the influence of

implementing AEL during constrained vertical jumping using computer modelling and simulation and examined whether the proposed mechanism of enhanced power, increased elastic energy storage and return, could enhance work and power.

Methods

We simulated human jumping motion with a simplified model, consisting of a ball-shaped body (head, arm, and trunk), two lower limb segments (thigh and shank), and four muscles. We adjusted the key activation parameters of the muscles to influence the performance outcome of the model. Numerical optimization was applied to search the optimal solution for the model. We implemented AEL and non-AEL conditions in the model to compare the simulated data between conditions.

Results

Our model predicted that the optimal jumping performance was achieved when the model utilized the whole joint range. However, there was no difference in jumping performance in AEL and non-AEL conditions because the model began its push-off at the similar state (posture, fiber length, fiber velocity, fiber force, tendon length, and the same activation level). Therefore, the optimal solution predicted by the model was primarily driven by intrinsic muscle dynamics (force-length-velocity relationship), and this coupled with the similar model state at the start of the push-off, resulting in similar push-off performance across all conditions. There was also no evidence of additional tendon-loading effect in AEL conditions compared to non-AEL condition.

Discussion

Our simulation results disagree with some experimental studies that reported increased jump performance with AEL. We suspect that, in some experimental studies, AEL's performance-enhancing effect might be caused by differences in activation strategies between those

47 undertaken by humans and those found through our model optimization, or due to the simplicity
48 of our model.

49 **Introduction**

50 During explosive movements, such as jumping and throwing, humans typically utilize stretch-
51 shortening cycles (SSC) by first performing an eccentric loading that aims to increase the force
52 and power in the subsequent concentric movement. Numerous studies on isolated muscles
53 (Cavagna & Citterio, 1974; Cavagna, Dusman, & Margaria, 1968; Cavagna, Saibene, &
54 Margaria, 1965) and *in vivo* human experiments (Bobbert, Gerritsen, Litjens, & van Soest, 1996;
55 Cronin, McNair, & Marshall, 2001; McBride, McCaulley, & Cormie, 2008; Sheppard, Newton,
56 & McGuigan, 2007) have confirmed that SSC can effectively increase the concentric force and
57 power output. However, the movement dynamics need to be precisely tuned so that interaction
58 between elastic and contractile elements in muscles enables maximization of power output
59 during the concentric phase of the movement (Ishikawa, Finni, & Komi, 2003; Ishikawa, Komi,
60 Finni, & Kuitunen, 2006).
61
62 Accentuated eccentric loading (AEL) is a form of movement manipulation that has been
63 suggested to enhance power output. AEL is a type of SSC that requires the person to perform a
64 heavy eccentric loading (added mass or force) followed by a light concentric loading. During the
65 AEL movement, the added external load is released at the transition from the eccentric to the
66 concentric phase. Some studies found that the acute response to AEL could increase jump height
67 by 4.3~9.52%, peak power output by 9.4~23.21%, and maximal concentric vertical ground
68 reaction force by 3.9~6.34% during a countermovement jump (Aboodarda, Yusof, Abu Osman,
69 Thompson, & Mokhtar, 2013; Sheppard et al., 2007). Similarly in bench press, Doan et al.

(2002) reported an increased concentric force and Ojasto and Häkkinen (2009) found increased concentric power. By contrast, Aboodarda et al. (2014) reported that AEL applied through elastic resistance during a drop jump did not alter jump height, muscle activation level, or other kinetics profiles during the concentric push-off phase. Indeed, a review study by Wagle et al. (2017) concluded that current evidence for both acute responses and chronic adaptation to AEL is inconsistent, possibly due to different exercises selected, training equipment used, or the load selected across different experiments. As a result, more research is needed to clarify the effects of AEL on force, work, and power production during explosive SSC movements.

There are a number of potential mechanisms that might drive enhanced power output during AEL movements. The most common explanation for why AEL should enhance power is that increased load amplifies elastic energy storage in the tendon and aponeurosis, which can then be released in the concentric phase (Wiesinger, Rieder, Kösters, Müller, & Seynnes, 2017). For instance, AEL countermovement jump may result in greater force generation in the descent to decelerate added inertia, potentially resulting in greater tendon loading prior to the upward motion. However, these effects on tendon loading or storage and return of energy are yet to be tested. At the whole-body level, one potential mechanism for enhanced performance is that AEL increases the net vertical impulse during the ground contact phase. This would increase take-off velocity and hence jump height. Bobbert et al. (1996) compared squat jump and CMJ performance and argued that CMJ conditions increased the ground contact time to build up a higher muscle force, which helped to increase the net vertical impulse, take-off velocity, and hence jump height. During AEL CMJ, the negative vertical impulse must be greater on the initial descent because the overall mass is greater than in non-AEL CMJ. However, the positive

93 impulse that is first generated to decelerate the greater mass must be also greater than the non-
94 AEL CMJ (net impulse must be zero at the bottom of the countermovement). Therefore, what is
95 unknown is whether the additional positive impulse that can be greater during the upward phase
96 (push-off) during AEL CMJ will be greater than without AEL. Whilst we might expect that
97 additional mass prior to release will increase force and hence vertical impulse in the upward
98 phase, this effect has yet to be examined.
99
100 Musculoskeletal modelling and simulation provide a powerful way to understand how AEL
101 might enhance power output. Simulation studies have suggested that the application of an
102 external load can result in MTU power amplification in some cases (Galantis & Woledge, 2003;
103 Sawicki, Sheppard, & Roberts, 2015). For example, when an intermediate external load was
104 applied to a Hill-type frog MTU model during stretch-shortening cycles or via a simulated catch
105 mechanism, MTU power was amplified above the maximal fibre power predicted from the
106 muscle's force-length-velocity relationship (Richards & Sawicki, 2012; Sawicki et al., 2015).
107 The extra MTU power was attributed to energy storage from the tendon. However, this effect
108 was highly sensitive to the effective mass, such that only a narrow optimal range of external load
109 magnitudes produced power amplification (Richards & Sawicki, 2012). Multi-segment
110 musculoskeletal simulations have also found that adding or removing weight impacts
111 performance of maximal effort jumps (Bobbert, 2014), however, the effect was smaller than that
112 reported in similar experimental studies (Markovic & Jaric, 2007; McBride, Haines, & Kirby,
113 2011; Pazin, Berjan, Nedeljkovic, Markovic, & Jaric, 2013). These simulation studies show that
114 applying additional load to the body can impact maximal task performance, and the magnitude of
115 the mass or resistance might be critical to allow this performance enhancement to occur. Among

the experimental studies that showed enhanced AEL jumping performance, the most common range of AEL loads was 15-30% body mass (Aboodarda, Page, & Behm, 2015; Aboodarda et al., 2013; Sheppard et al., 2007). To date, however, there have been no simulation studies exploring how sudden manipulation of loads applied during a movement, as per AEL protocols, might enhance work or power output from the musculoskeletal system.

The primary aim of this study was to use simulations to explore how AEL influences muscle work and power during a jumping task. We chose a simplified model to examine whether additional load during the eccentric phase of movement enhances muscle performance via elastic tendon-loading mechanics, without confounding effects of changes in body posture, joint coordination and range of motion. Our simplified biomimetic mechanical system constrained movement of the trunk, and consisted of only two segments (representing the tight and shank) and was powered by four muscles acting around the hip and knee joints. The AEL conditions tested in our simulations were 15% and 30% additional body mass. We hypothesised that AEL would enhance work and power compared to simulations in which mass did not change in our model.

Materials & Methods

Model Details

Our simulations were performed using OpenSim 4.0 software (Delp et al., 2007; Seth et al., 2018). We performed two-dimensional forward dynamic simulations (*Fig. 1*). The model consisted of a body representing the head, arms, and trunk (HAT) and two rigid segments representing the thigh and shank.

The HAT segment was constrained so that it only moved in the vertical direction with no rotational degree-of-freedom. HAT, thigh, and shank segments were connected by hinge joints representing the hip and knee. The joints were only allowed to move freely within a specified range (hip = 0°~90° hip flexion, knee = 0°~135° knee flexion, zero represents the joint angle at upright posture, positive value represents the direction of joint flexion). Joint range was constrained by applying a spring-damper model that applied a resistive torque in proportion to the change of angular velocity beyond the prescribed range. This spring-damper model had an equivalent function to the passive anatomical structures that stabilize the joint (i.e. ligaments and joint capsules), and the parameters in the spring-damper model are provided in *Table 1*.

The model's mass, inertial properties and segment lengths (*Table 1*) were adapted from the 10-segment, 23 degree-of-freedom model developed by Anderson and Pandy (1999). The mass and inertial properties of HAT include all segments from pelvis and above. The mass of the thigh and shank segments were twice those in Anderson and Pandy (1999), in order to represent two legs combined. The mass and inertial properties were all scaled to one subject (height: 1.78 m, mass: 78 kg), and the segment lengths were also taken from the same subject. We added a Hunt-Crossley contact model to define the contact points between the model and ground (Hunt & Crossley, 1975), with values tuned to ensure that there was no premature take-off of the model during descent and limited sliding of contact spheres. Parameters are provided in *Table 1*.

Muscle Actuators

We used four different muscle-tendon-unit (MTU) actuators to represent the major muscles in the lower limb. These MTU actuators were based on a three element Hill-type muscle model (Zajac, 1989). These MTU actuators were the vasti muscle groups (VAS), rectus femoris (REC), gluteus maximus (GLU), hamstring muscle groups (HAM). The Opensim muscle model used in our simulation was the Millard2012EquilibriumMuscle model (Millard, Uchida, Seth, & Delp, 2013). The input to the model was muscle excitation, which represented the excitatory signal from the peripheral nervous system that activated the muscle. Muscle excitation ranged between 0 and 1, which also led to muscle activation in the model via a first-order differential equation representing excitation-contraction coupling (Millard et al., 2013).

Muscle Parameters

The muscle parameters were adapted from the leg muscle model by Delp et al. (1990). Maximal isometric force (F_{max}) of each muscle was scaled to the power of 2/3 relative to the scale factor applied to mass and inertial scaling. This was based on the scaling relationship between segment mass and segment cross-sectional area, assuming uniform segment density. F_{max} of each muscle was then doubled so that it matched the force generated by both legs. Our muscle model assumed no pennation angle for simplicity. We modified L_{opt} and L_{tendon} so that the passive tension from the muscle did not exceed 5% of the F_{max} value during the model's constrained jumping motion. The muscle parameters are provided in *Table 2*.

Model Excitation

At the start of each simulation, the model was set at an initial posture at 5° hip flexion, 10° knee flexion such that the HAT segment would fall, and the knee and hip joints would flex, due to

gravity. All muscles began the simulation with the minimum muscle excitation of 0.01. The initial muscle activation was set to 0.01 for all muscles. We did not specify the initial fibre length, instead Opensim computed fibre length based on the initial muscle activation and other muscle parameters detailed in Table 2 (equilibration occurring at start of simulation). Muscle excitation remained at 0.01 until the *excitation onset* for each muscle, after which time the excitation increased to a maximum value of 1 with an excitation rate or *slope of excitation* between 1/s and 10/s. Therefore, the model's motion was determined by the interaction between the *excitation onset* and *slope of excitation* (*Fig. 2*) of each muscle and the passive mechanics of the model. An optimization (details below) was run to determine the optimal combination of muscle excitation onsets and slope of excitations to achieve the maximum jump height in each model. We set the duration of the simulation to 1.7 seconds to ensure sufficient time for the model to reach the highest point in the airborne phase.

Cost Function and Optimization Routine

The primary cost function was based on maximizing jump height, however there was also a penalization term. To prevent the model utilizing the spring properties set to mimic passive joint structures at the end of range for each joint, we penalised such motion (assuming excessive flexion/extension is not desirable due to the likelihood of injury). In each simulation, the joint limit for the knee (135° knee flexion) at the bottom of the squat was used as the kinematic penalty term in the cost function. Given the geometry of the model, the hip joint would never reach its joint range throughout the jumping motion until take-off, and therefore was not included in the penalty term.

The optimization criteria were: (1) maximize jump height, (2) minimize knee joint limit penalization term. The weights for each parameter were determined to ensure that minimum spring-damper torque was applied during the movement, whilst ensuring jump height was prioritised. The weights were hand-tuned with arbitrary values on a trial-and-error basis. Jump height was defined as the difference in HAT centre of mass position between the model's initial posture and the highest position achieved in the simulation. The optimization cost function (J) is provided below, where H represents jump height and θ represents maximal knee angle in the jump:

$J = H - 0.01 \times (\theta - 135°)$, or

$J = H$, if $\theta < 135°$

The numerical optimization was performed in MATLAB (version R2018b; MathWorks, Natick, United States). We used a nonlinear simplex algorithm "fminsearchbnd" (D'Errico, 2020) to search the optimal solution for our cost function within bounds given above. "fminsearchbnd" is an extension of MATLAB "fminsearch" algorithm, but it also accommodates the parameter bounds of all input variables when searching for global minimum. To find the global maximum of our cost function, we multiplied our cost function by -1 so that the minimum value from "fminsearchbnd" represented the maximum value of the cost function.

There were three conditions to be optimized: the normal condition, a 15% AEL condition, and a 30% AEL condition. In the normal condition, the model mass was kept at the original mass (*Table 1*) to represent a standard countermovement jump without external load. In AEL conditions, there were two steps involved in the optimization process (termed 'split' method). In

step 1, we performed an optimization search of the cost function provided above with 15% and 30% additional body mass added to the model (added to HAT segment), and the parameters to be optimized were muscle excitation onsets and slope of excitations. After finding the optimal solution for each added mass, step 2 involved starting a new simulation from the beginning of upward motion with the added mass removed from the model to simulate the AEL concentric condition. The exact states [muscle excitations, muscle fibre and tendon lengths and joint position and velocity] at the beginning of upward motion in step 1 were implemented at the start of the simulation of step 2. A new optimisation of muscle excitation parameters during step 2 was conducted, as some muscles may not have been excited during the optimisation in step 1. We approximated the beginning of upward motion as the time when the VAS fiber velocity became zero and hence started generating positive work. Originally, we used the lowest COM height to determine the turning point of the simulation. However, to reduce discontinuities in muscle forces that occurred across the split simulations, we instead approximated this turning point via VAS fiber kinematics. We found that the time when fiber velocity approached zero occurred at a very similar time to the model's turning point (0.0201 and 0.0206 seconds difference for 15% and 30% AEL conditions), with limited discontinuity. We then compared the muscle and model dynamics during upward motion (i.e. push-off phase) in three different conditions.

We used a "split" method because we were unable to perform a simulation that changed the model's mass halfway through the movement in the Opensim platform. Whilst it is possible to add an external force in the descent phase of movement and removed this external force during ascent, this solution does not account for the effect of inertia during the descent. The "split"

method assumes that the optimal AEL jump (added mass removed at the turning point) shares the same eccentric portion of the optimal jump with added mass (executed to completion). While this assumption may not be true of jumping humans, who may select different squat depths or rates of descent between AEL and added mass jumps, our purpose here was to exclude effects like change of squat depth so that we could examine the fundamental fibre-tendon mechanics differences between AEL and non-AEL conditions in isolation. The maximum jump achieved under all weight conditions always occurred for the deepest squat possible, where force is applied through the maximum range. As such it seems that this is a fair comparison of optimal jumping across conditions.

Simulation Data Analysis

Squat depth was defined as the difference in HAT centre of mass position between the model's initial posture and the lowest position achieved in the simulation. Muscle power was calculated as muscle work divided by push-off time, and therefore was the average power during push-off. The push-off time was defined as the time for the HAT centre of mass to move from the beginning of upward motion until take-off.

The total muscle work in the model did not necessarily equate to the effective vertical work done on the whole system. This is because some ineffective energy was expended during the jumping motion, such as the horizontal and rotational kinetic energy of each segment. To understand how AEL affected the whole system dynamics, the model's vertical ground reaction force (VGRF), center of mass (COM) vertical velocity, and COM vertical power were calculated. The vertical component of the Hunt-Crossley contact force between the model and the ground was taken as

the VGRF. The COM vertical power was calculated as the product of the VGRF and the COM vertical velocity, and only the push-off phase was analyzed.

Results

Squat Depth

The AEL conditions achieved a similar squat depth to the normal condition (less than 0.5% difference in squat depth). Consequently, the joint ranges produced by the model did not differ meaningfully across conditions, which means that any performance difference found in different conditions was not simply caused by the movement range.

Muscle Work and Power

The muscle work and power contributions during the push-off phase are provided in *Fig. 3*. The individual and total (i.e. sum of all muscles) muscle works and powers are compared across normal, 15% AEL, and 30% AEL conditions as the percentage difference relative to the normal (no AEL) condition. Both high and low AEL conditions showed a negligible change in total muscle work (less than 1% reduction) compared to the normal condition. Since our model achieved similar squat depths across conditions, the total muscle work during the push-off phase primarily determined the effective jump height in our model. We found a negligible change in effective jump height (less than 1% reduction) in both AEL conditions compared to the normal condition (*Table 3*). The major finding was that AEL did not increase total muscle work or effective jump height in our model.

298 *Figure 3* shows an overall small increase in total muscle power in AEL conditions compared to
299 the normal condition, with the percentage increase slightly higher in the 15% AEL condition
300 compared to the 30% AEL condition. Nevertheless, the percentage increase was less than 3%,
301 which might be considered a relatively small effect for average muscle power, noting that this
302 did not cause an increase in jump height.
303
304 **Whole System Dynamics**
305 The relative differences in peak VGRF and peak COM vertical power during push-off between
306 AEL conditions and the normal condition are summarized in *Table 4*. Our model showed
307 negligible changes (less than 1% reduction) in peak VGRF and peak COM vertical power.
308 Furthermore, the VGRF and COM vertical power curves relative to time are very similar in
309 shape (*Fig. 4*), which also explains why our model had negligible change in effective jump
310 height (less than 1%).
311
312 **Dynamics of Muscle**
313 Given that the jumping motion was primarily knee-dominant, we use the results from the VAS
314 muscle-tendon dynamics to explore why there was a lack of AEL improvement in muscle work,
315 muscle power, and the whole system dynamics. *Figure 5* shows the activation, MTU force,
316 tendon length, fiber length, and fiber velocity for VAS for the entire jumping motion (optimized)
317 across three different loading conditions. The 30% AEL condition showed the earliest increase in
318 VAS activation, followed by the 15% AEL condition, and then the normal condition. This
319 allowed the 30% AEL condition to produce the required active muscle force in the descending
320 phase with sufficient time to decelerate the system's COM before the end of joint range (which

would otherwise be penalized in the optimization cost function). As a consequence, VAS MTU force was higher than in the normal condition during the descending phase in both AEL conditions (*Fig. 5*).

Prior to achieving the model's lowest position, VAS was already at full activation across all three conditions (*Fig. 5*). Peak activation occured at approximately the middle of eccentric phase, and force then decreased until the lowest point in the movement such that the VAS MTU force at the start of the push-off differed by less than 0.1% between AEL and normal conditions. The VAS tendon length (less than 0.001% difference), fiber length and fibre velocity (less than 0.05% difference) also had similar magnitudes across three different conditions at the start of the push-off (*Fig. 5*). Therefore, this analysis shows that each condition resulted in very similar states at the start of the push-off phase, regardless of added mass in the AEL conditions. The model in AEL conditions therefore behaved similarly to the normal condition during push-off.

Discussion

This simulation study explored the mechanisms of putative work and power enhancement due to AEL during jumping. Our major findings contradicted our orginal hypothesis. We found that neither AEL load condition increased total muscle work or effective jump height during an optimal constrained countermovement jump. Our simulations actually showed slight reductions in performance (<1%), which differed from the *in vivo* studies that reported 4.3~9.52% increases in effective jump height by utilizing AEL (Aboodarda et al., 2013; Sheppard et al., 2007). We also found that our model had negligible difference (less than 1%) in peak VGRF and peak COM vertical power during push-off across conditions, contrasting with *in vivo* studies that reported

3.9~6.34% increases in maximal concentric vertical ground reaction force, and 9.4~23.21% increases in peak concentric power output by utilizing AEL (Aboodarda et al., 2013; Sheppard et al., 2007).

We also found that the agonist muscles (VAS and REC) generated slightly less muscle work in the AEL conditions, which contributed to slightly less COM work and jump height. However, the push-off duration was also shorter in the AEL conditions, contributing to a slightly higher muscle power despite a minimal reduction in muscle work. The changes in jump height and muscle power in AEL conditions were minimal, and are best interpreted as being no different between conditions.

The results indicate that the lack of difference in jump performance was a result of the states of the system being equivalent at the bottom of the movement, despite differences in the weight of the model/system at this point. Our results showed that our model descended to a similar squat depth to ensure the whole joint range was fully utilized in the push-off phase, regardless of the conditions. Thus, our model began push-off at a similar posture, similar fiber length and fiber velocity, similar tendon length, similar fiber force, and the same (i.e. complete) activation level. Therefore, the optimal solution predicted by our model was primarily driven by intrinsic muscle dynamics (force-length-velocity relationship), and this coupled with the similar model state at the start of the push-off led to similar push-off performance across all conditions. The reason the states were equivalent at the release point of the weights (beginning of push-off) seems to be that the optimal solution required that the muscle achieved its full activation prior to the bottom of the movement to utilize maximum muscle and tendon work on the ascent. As such, at the bottom

of the movement (with the same joint angle across conditions), the maximum force was dictated by the maximum force capability of a maximally activated muscle, and this was equivalent in different conditions.

One explanation that has been proposed as a potential mechanism for enhanced performance in AEL is storage of elastic energy in tendons. In this regard, it is important to remember that tendon length is a function of MTU force. Our simulations showed that AEL conditions caused a larger tendon excursion during the descending phase (*Fig. 5*). However, the additional elastic energy stored in the tendon was already returned to the system before the model achieved its lowest posture. This returned elastic energy from the tendon was absorbed into the contractile element (or muscle fibers) prior to achieving the lowest position, demonstrated by the shortening of the VAS tendon (as force declined) while the MTU continued to lengthen via fibre (contractile) lengthening (Fig. 5). As a result, there was no difference in the stored elastic energy between different conditions when compared at the bottom of the movement. In other words, our constrained jumping model predicted the same available elastic energy to be returned into the push-off phase, and therefore our proposed tendon-loading mechanism did not facilitate an increase in elastic energy in AEL conditions compared to normal conditions. The reason our simulations found this unique movement strategy was because the optimizer only searched the movement solution producing the highest jump height, and this unique strategy was the best solution given the constraints of the model. Storing elastic energy in the tendon was not the criteria of the optimization process, and therefore the optimizer did not account for this factor.

389 There might be concern over whether the model gave sufficient validity to explore the AEL
390 jumping movements because of the simplicity of the model. To address this major concern, we
391 compared our simulated jump height results to the ranges measured in the literatures that
392 included trunk constraints during human jumping (Kubo et al., 2007; Pérez-Castilla, McMahon,
393 Comfort, & García-Ramos, 2020), which were reported to be around 20 cm. Considering that our
394 model removed the foot segment and ankle joint rotation, the values from our model (around 10
395 cm) was a good approximation of the knee-dominant motion. We also examined the general
396 timing of muscle activation during human jumping (Held et al., 2020; Padulo et al., 2013) and
397 found that vastus EMG achieved close to maximum value at the bottom of the jump, and the
398 biceps femoris EMG achieved maximum value after take-off. These EMG activation patterns
399 were similar to the results of our model. Considering the fact that the model found the deepest
400 squat depth as the optimum solution, this demonstrates our model operates in a similar (albeit
401 abstract) way to the human body during jumping (Sánchez-Sixto, Harrison, & Floría, 2018).
402
403 There are some limitations to interpreting the findings based on our modelling assumptions.
404 Firstly, our model assumed a 'bang-bang' muscle control towards maximal excitation, and
405 therefore the muscles were not allowed to use submaximal activation after the excitation slope
406 finished ramping up. Muscle control in the human musculoskeletal system is often more complex
407 than that described by a simple bang-bang assumption. EMG characteristics have been shown
408 not to differ between AEL and body-weight drop jumps during push-off (Aboodarda et al.,
409 2014), however not all muscles are likely to be fully active prior to the upward propulsion phase
410 of jumping (Bobbert et al., 1996), in contrast to the simulations specified by our optimal
411 solution. In reality, different muscles may achieve different activation levels over time during

412 human jumping and the bang-bang muscle control used in the simulation may have limited our
413 model's representativeness, because it did not accurately simulate a human-like muscle
414 activation. However, all optimal solutions in our simulation specified maximum muscle
415 activation prior to upward movement and hence it is likely that this is the optimal method in our
416 simplified model, regardless of how the muscle gets to this activation level. In another jumping
417 simulation study with more complicated muscle control (i.e. step function), the mono-articular
418 muscles still produced the similar activation pattern while some bi-articular muscles behaved
419 differently (i.e. REC activation ramped up after push-off began) (Nagano, Komura, & Fukashiro,
420 2007). Our simulations also found the lowest squat depth to be the optimal solution, whereas real
421 humans don't necessarily utilize the deepest squat depth when performing a self-selected
422 maximal jump (Mandic, Jakovljevic, & Jaric, 2015). Although previous simulation studies have
423 also shown that increasing squat depth should improve maximal jump height (Bobbert, Casius,
424 Sijpkens, & Jaspers, 2008; Domire & Challis, 2007), this relationship has not been observed in
425 human experiments in which healthy adults and elite athletes participated (Domire & Challis,
426 2007; Mandic et al., 2015). Possible explanations to avoid theoretically optimal deeper squat
427 depths include joint discomfort and joint protective mechanisms. Another physiological property
428 of the muscle not considered in our model is residual force enhancement (Hahn, Seiberl,
429 Schmidt, Schweizer, & Schwirtz, 2010). Residual force enhancement increases the muscle force
430 after the lengthening of the muscle fibre (Hahn et al., 2010). As a result, stretch-shortening cycle
431 (SSC) movements might benefit from residual force enhancement and hence power
432 enhancement. Residual force enhancement was not simulated in our muscle model, adding
433 another limitation to our study. However, when examining gross movement tasks, residual force
434 enhancement has been found to have little or no effect on the magnitude of force production

(Brown & Loeb, 2000). Therefore, residual force enhancement observed at the single muscle is unlikely to contribute significantly to the force enhancement during a multi-joint, multi-muscle SSC. Finally, we did not test the effect of adding a foot segment with multiple contact points, which allows the centre of pressure to translate. However, we expect that the results will be similar with more complex models, providing the optimal solution requires that muscles are maximally active prior to take-off.

It is important to consider why AEL may cause work and power enhancement in some human experiments (Aboodarda et al., 2013; Sheppard et al., 2007), but not in our simulations. Sheppard et al. (2007) reported the same squat depth being selected by the participants with improved jump height under AEL conditions. With the same squat depth, any difference in work, power, or jump height during the push-off phase can only be determined by the force produced by the muscle, but not the joint range. Sheppard et al. (2007) proposed that AEL may have caused a higher muscle force at the initiation of the upward velocity to cause work enhancement. However, our simulations predicted that the highest muscle force occurred before the model achieved the lowest position, and that the muscle force was similar at the initiation of the upward acceleration across different added load (AEL) conditions. We believe that the discrepancy between these in-vivo data and our simulation findings most likely occurred because our control scheme (bang-bang) is different to that employed biologically. It remains to be seen, however, why humans don't adopt the optimal solution that requires maximum muscle activation prior to upward movement. Potentially, activation is sub-optimal without AEL during actual CMJ, and AEL changes mechanics/activation patterns to improve jumping performance. It could be argued that our model is already maximising the storage and generation of energy (i.e. full activation

and same states at turning point), and hence AEL can't improve performance further. An alternative view is that humans are able to find an optimal solution that our model cannot because humans achieve greater jump heights with AEL. Maybe, if our model could find the optimal control strategy that humans use, our solution would be able to make more use of energy stored in tendon. As such, we suspect that in-vivo findings of superior performance with AEL compared to normal jumping may be attributed to neural control factors, which might (or might not) produce a movement pattern that stores and returns more elastic energy in the tendon.

Conclusions

In this simulation study, we found that countermovement jump performance (i.e. jump height, COM vertical power) did not improve with AEL, irrespective of the magnitude of added load. This lack of effect primarily occurred because both AEL and non-AEL conditions had the same squat depth, muscle activation level, and muscle/tendon force at the start of the upward motion. Since AEL did not change model tendon strain at the start of the push-off phase, it did not affect the amount of stored elastic energy available for return in the push-off phase. Therefore, our results highlight that AEL does not take advantage of a potential tendon-loading effect to enhance work and power output in our optimised simulation. Our findings assumed that the major lower limb muscles already achieved and were able to maintain full activation throughout the push-off phase. However, utilizing bang-bang muscle control might have mis-represented human jumping control, and therefore our findings provide only theoretical evidence that altering mechanical loading in a simple but highly constrained musculoskeletal system does not affect effective work and power output. Changing the muscles' activation profiles might alter how

elastic energy interacts within the jumping system; however, more research is still needed to explore this speculation.

Acknowledgements

We gratefully thank Dr. Matthew Millard (Heidelberg University) in providing technical assistance and suggestions in developing our modelling and simulation protocols.

References

Aboodarda, S. J., Byrne, J. M., Samson, M., Wilson, B. D., Mokhtar, A. H., & Behm, D. G. (2014). Does performing drop jumps with additional eccentric loading improve jump performance ? *Journal of Strength and Conditioning Research, 28*(8), 2314-2323.

Aboodarda, S. J., Page, P. A., & Behm, D. G. (2015). Eccentric and concentric jumping performance during augmented jumps with elastic resistance: A meta-analysis. *International Journal of Sports Physical Therapy, 10*(6), 839-849.

Aboodarda, S. J., Yusof, A., Abu Osman, N. A., Thompson, M. W., & Mokhtar, A. H. (2013). Enhanced performance with elastic resistance during the eccentric phase of a countermovement jump. *International Journal of Sports Physiology and Performance, 8*(2), 181-187.

Anderson, F. C., & Pandy, M. G. (1999). A dynamic optimization solution for vertical jumping in three dimensions. *Computer Methods in Biomechanics and Biomedical Engineering, 2*(3), 201-231.

Bobbert, M. F. (2014). Effect of unloading and loading on power in simulated countermovement and squat jumps. *Medicine and Science in Sports and Exercise, 46*(6), 1176-1184.

Bobbert, M. F., Casius, L. J., Sijpkens, I. W., & Jaspers, R. T. (2008). Humans adjust control to initial squat depth in vertical squat jumping. *Journal of Applied Physiology, 105*(5), 1428-1440.

Bobbert, M. F., Gerritsen, K. G., Litjens, M. C., & van Soest, A. J. (1996). Why is countermovement jump height greater than squat jump height ? *Medicine and Science in Sports and Exercise, 28*(11), 1402-1412.

Brown, I. E., & Loeb, G. E. (2000). Measured and modeled properties of mammalian skeletal muscle: III. the effects of stimulus frequency on stretch-induced force enhancement and shortening-induced force depression. *Journal of Muscle Research and Cell Motility, 21*, 21-23.

Cavagna, G. A., & Citterio, G. (1974). Effect of stretching on the elastic characteristics and the contractile component of frog striated muscle. *Journal of Physiology, 239*(1), 1-14.

Cavagna, G. A., Dusman, B., & Margaria, R. (1968). Positive work done by a previously stretched muscle. *Journal of Applied Physiology, 24*(1), 21-32.

Cavagna, G. A., Saibene, F. P., & Margaria, R. (1965). Effect of negative work on the amount of positive work performed by an isolated muscle. *Journal of Applied Physiology, 20*, 157-158.

Cronin, J. B., McNair, P. J., & Marshall, R. N. (2001). Magnitude and decay of stretch-induced enhancement of power output. *European Journal of Applied Physiology, 84*(6), 575-581.

Delp, S. L., Anderson, F. C., Arnold, A. S., Loan, P., Habib, A., John, C. T., . . . Thelen, D. G. (2007). OpenSim: Open-source software to create and analyze dynamic simulations of movement. *IEEE Transactions on Biomedical Engineering, 54*(11), 1940-1950.

Delp, S. L., Loan, J. P., Hoy, M. G., Zajac, F. E., Topp, E. L., & Rosen, J. M. (1990). An interactive graphics-based model of the lower extremity to study orthopaedic surgical procedures. *IEEE Transactions on Biomedical Engineering, 37*(8), 757-767.

Doan, B. K., Newton, R. U., Marsit, J. L., Triplett-McBride, N. T., Koziris, L. P., Fry, A. C., & Kraemer, W. J. (2002). Effects of increased eccentric loading on bench press 1RM. *Journal of Strength and Conditioning Research, 16*(1), 9-13.

Domire, Z. J., & Challis, J. H. (2007). The influence of squat depth on maximal vertical jump performance. *Journal of Sports Sciences, 25*(2), 193-200.

Galantis, A., & Woledge, R. C. (2003). The theoretical limits to the power output of a muscle-tendon complex with inertial and gravitational loads. *Proceedings of the Royal Society B: Biological Sciences, 270*(1523), 1493-1498.

Hahn, D., Seiberl, W., Schmidt, S., Schweizer, K., & Schwirtz, A. (2010). Evidence of residual force enhancement for multi-joint leg extension. *Journal of Biomechanics, 43*(8), 1503-1508.

Held, S., Siebert, T., & Donath, L. (2020). Electromyographic activity of the vastus medialis and gastrocnemius implicates a slow stretch-shortening cycle during rowing in the field. *Scientific Reports, 10*, 9451.

Hunt, K. H., & Crossley, F. R. E. (1975). Coefficient of restitution interpreted as damping in vibroimpact. *Journal of Applied Mechanics, 42*(2), 440-445.

Ishikawa, M., Finni, T., & Komi, P. V. (2003). Behaviour of vastus lateralis muscle-tendon during high intensity SSC exercises in vivo. *Acta Physiologica Scandinavica, 178*(3), 205-213.

Ishikawa, M., Komi, P., Finni, T., & Kuitunen, S. (2006). Contribution of the tendinous tissue to force enhancement during stretch–shortening cycle exercise depends on the prestretch and concentric phase intensities. *Journal of Electromyography and Kinesiology, 16*(5), 423-431.

Kubo, K., Morimoto, M., Komuro, T., Tsunoda, N., Kanehisa, H., & Fukunaga, T. (2007). Influences of tendon stiffness, joint stiffness, and electromyographic activity on jump performances using single joint. . *European Journal of Applied Physiology 99*(3), 235-243.

Mandic, R., Jakovljevic, S., & Jaric, S. (2015). Effects of countermovement depth on kinematic and kinetic patterns of maximum vertical jumps. *Journal of Electromyography and Kinesiology, 25*(2), 265-272.

Markovic, G., & Jaric, S. (2007). Positive and negative loading and mechanical output in maximum vertical jumping. *Medicine and Science in Sports and Exercise, 39*(10), 1757-1764.

McBride, J. M., Haines, T. L., & Kirby, T. J. (2011). Effect of loading on peak power of the bar, body, and system during power cleans, squats, and jump squats. *Journal of Sports Sciences, 29*(11), 1215-1221.

McBride, J. M., McCaulley, G. O., & Cormie, P. (2008). Influence of preactivity and eccentric muscle activity on concentric performance during vertical jumping. *Journal of Strength and Conditioning Research, 22*(3), 750-757.

Millard, M., Uchida, T., Seth, A., & Delp, S. L. (2013). Flexing computational muscle: Modeling and simulation of musculotendon dynamics. *Journal of Biomechanical Engineering, 135*(2), 021005.

Nagano, A., Komura, T., & Fukashiro, S. (2007). Optimal coordination of maximal-effort horizontal and vertical jump motions – a computer simulation study. *BioMedical Engineering OnLine, 6*(20).

Ojasto, T., & Häkkinen, K. (2009). Effects of different accentuated eccentric load levels in eccentric-concentric actions on acute neuromuscular, maximal force, and power responses. *Journal of Strength and Conditioning Research, 23*(3), 996-1004.

Padulo, J., Tiloca, A., Powell, D., Granatelli, G., Bianco, A., & Paoli, A. (2013). EMG amplitude of the biceps femoris during jumping compared to landing movements. *SpringerPlus, 2*, 520.

Pazin, N., Berjan, B., Nedeljkovic, A., Markovic, G., & Jaric, S. (2013). Power output in vertical jumps: Does optimum loading depend on activity profiles? *European Journal of Applied Physiology, 113*(3), 577-589.

Pérez-Castilla, A., McMahon, J. J., Comfort, P., & García-Ramos, A. (2020). Assessment of loaded squat jump height with a free-weight barbell and smith machine: Comparison of the takeoff velocity and flight time procedures. *Journal of Strength and Conditioning Research, 34*(3), 671-677.

Richards, C. T., & Sawicki, G. S. (2012). Elastic recoil can either amplify or attenuate muscle-tendon power, depending on inertial vs. fluid dynamic loading. *Journal of Theoretical Biology, 313*, 68-78.

Sánchez-Sixto, A., Harrison, A. J., & Floría, P. (2018). Larger countermovement increases the jump height of countermovement jump. *Sports, 6*(4), 131.

Sawicki, G. S., Sheppard, P., & Roberts, T. J. (2015). Power amplification in an isolated muscletendon unit is load dependent. *Journal of Experimental Biology, 218*, 3700-3709.

Seth, A., Hicks, J. L., Uchida, T. K., Habib, A., Dembia, C. L., Dunne, J. J., . . . Delp, S. L. (2018). OpenSim: Simulating musculoskeletal dynamics and neuromuscular control to study human and animal movement. *PLOS Computational Biology, 14*(7), e1006223. Retrieved from https://doi.org/10.1371/journal.pcbi.1006223

Sheppard, J., Newton, R., & McGuigan, M. (2007). The effect of accentuated eccentric load on jump kinetics in high-performance volleyball players. *International Journal of Sports Science and Coaching, 2*(3), 267-273.

Wagle, J., Taber, C., Cunanan, A., Bingham, G., Carroll, K., DeWeese, B., . . . Stone, M. (2017). Accentuated eccentric loading for training and performance: A review. *Sports Medicine, 47*(12), 2473-2495.

Wiesinger, H. P., Rieder, F., Kösters, A., Müller, E., & Seynnes, O. R. (2017). Sport-specific capacity to use elastic energy in the patellar and Achilles tendons of elite athletes. *Frontiers in Physiology, 8*, 132.

Zajac, F. E. (1989). Muscle and tendon: Properties, models, scaling, and application to biomechanics and motor control. *Critical Reviews in Biomedical Engineering, 17*(4), 359-411.

Table 1(on next page)

Model parameters

Table 1:
Model parameters

Segmental properties of the model's segments			
	Mass (kg)	**Moment of Inertia (kg.m^2)**	**Diameter (m) or Length (m)**
Ball-shaped Body (HAT)	47.64	1.482	0.15
Thigh Segment	19.44	0.146	0.4
Shank Segment	7.68	0.053	0.4
Hunt-Crossley parameters		**Spring-damper parameters**	
Stiffness (N/m)	10^7	Upper Stiffness (N.m/degree)	10
Dissipation	20	Lower Stiffness (N.m/degree)	1
Static coefficient of friction	2	Transition (degree)	3.0
		Damping (N.m/degree/s)	100

Table 2(on next page)

Muscle parameters

1

Table 2:
Muscle parameters

	F_{max} (N)	L_{opt} (m)	L_{tendon} (m)
VAS	9272	0.1765	0.2065
REC	2393	0.1766	0.3144
GLU	3888	0.0671	0.0679
HAM	6796	0.1166	0.3584

2

3

4

5

Table 3(on next page)

Relative difference in effective jump height between AEL conditions and the normal condition (chosen as baseline).

Negative sign in AEL conditions denotes decrease in effective jump height compared to baseline.

Table 3:
Relative difference in effective jump height between AEL conditions and the normal condition (chosen as baseline).
Negative sign in AEL conditions denotes decrease in effective jump height compared to baseline.

Normal	baseline
15% AEL	-0.798%
30% AEL	-0.899%

1

Table 4(on next page)

Percentage difference in peak VGRF and peak COM vertical power during push-off between AEL conditions and normal condition (chosen as baseline).

Positive / negative sign denotes the increase / decrease in value compared to baseline.

Table 4:
Percentage difference in peak VGRF and peak COM vertical power during push-off between AEL conditions and normal condition (chosen as baseline).
Positive / negative sign denotes the increase / decrease in value compared to baseline.

	Condition	Percentage difference
Peak VGRF (N)	Normal	baseline
	15% AEL	-0.16%
	30% AEL	-0.12%
Peak COM vertical power (W)	Normal	baseline
	15% AEL	-0.13%
	30% AEL	-0.07%

1

2

Figure 1

Four muscles model to perform two-dimensional forward dynamic simulation.

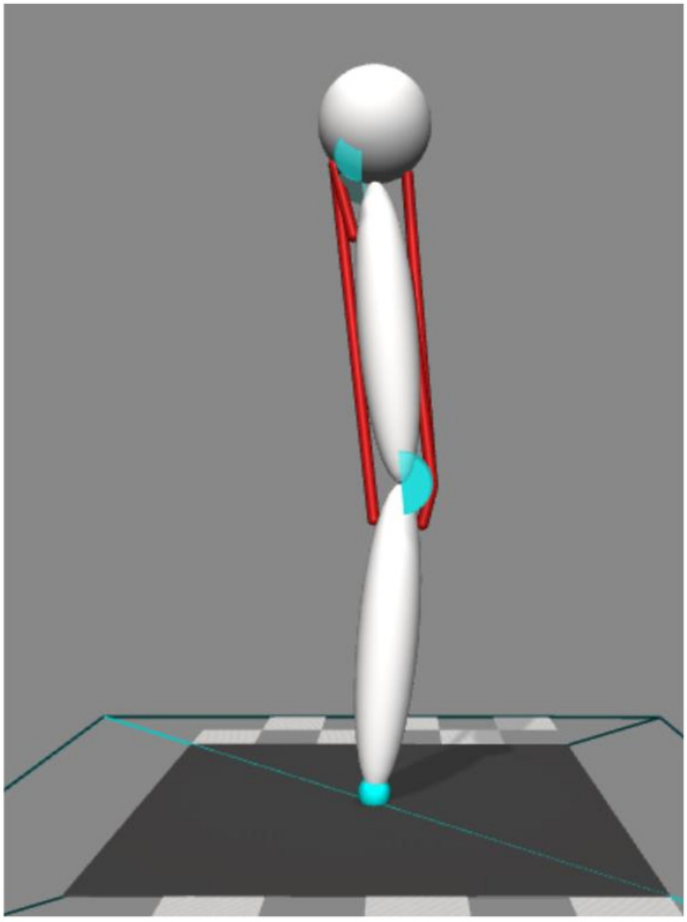

Figure 2

Example of one combination of “excitation onset” and “slope of excitation."

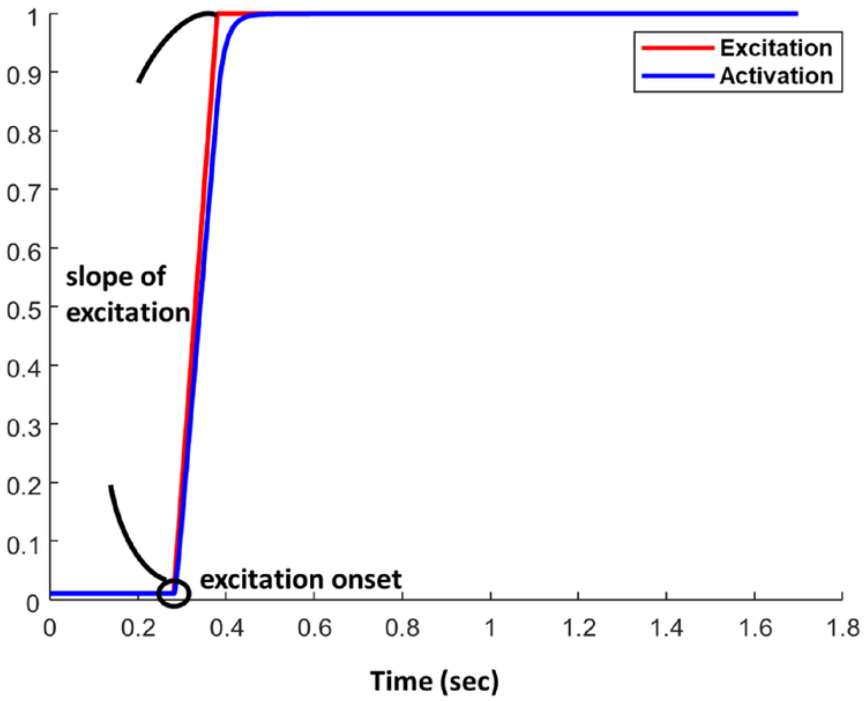
Excitation
Activation
slope of
excitation
excitation onset
Time (sec)
0
0.1
0.2
0.3
0.4
0.5
0.6
0.7
0.8
0.9
1
0.2
0.4
0.6
0.8
1.2
1.4
1.6
1.8

Figure 3

Muscle work and power during push-off phase across normal, 15% AEL, and 30% AEL conditions.

The percentage values above bars denotes the relative change from the corresponding normal condition. Positive sign represents increased work and power, and negative sign represents decreased work and power.

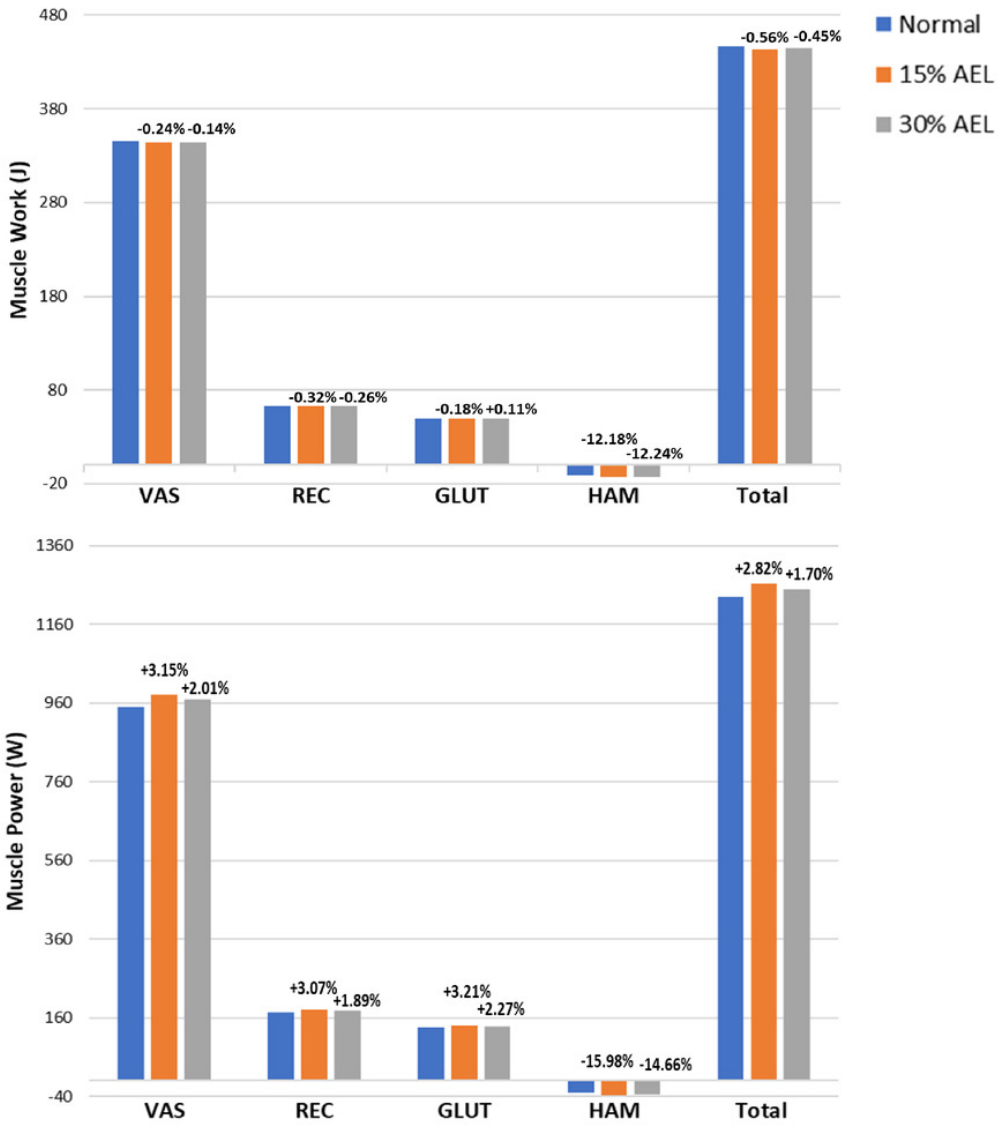
Normal
15% AEL
30% AEL
Muscle Work (J)
480
380
280
180
80
-20
-0.24% -0.14%
-0.32% -0.26%
-0.18% +0.11%
-12.18%
-12.24%
-0.56% -0.45%
VAS
REC
GLUT
HAM
Total
Muscle Power (W)
1360
1160
960
760
560
360
160
-40
+3.15%
+2.01%
+3.07%
+1.89%
+3.21%
+2.27%
-15.98%
-14.66%
+2.82%
+1.70%
VAS
REC
GLUT
HAM
Total

Figure 4

Force, velocity, and power profile representing the whole system dynamics across normal, 15% AEL, and 30% AEL conditions.

The graph in the left column shows the VGRF for the entire jumping motion until take-off. The color-filled markers represents the time when the model achieved the lowest posture. Three different conditions were time-normalized from the lowest posture to take-off. The three graphs in the right column show the time-normalized VGRF, COM vertical velocity, and COM vertical power during the push-off phase.

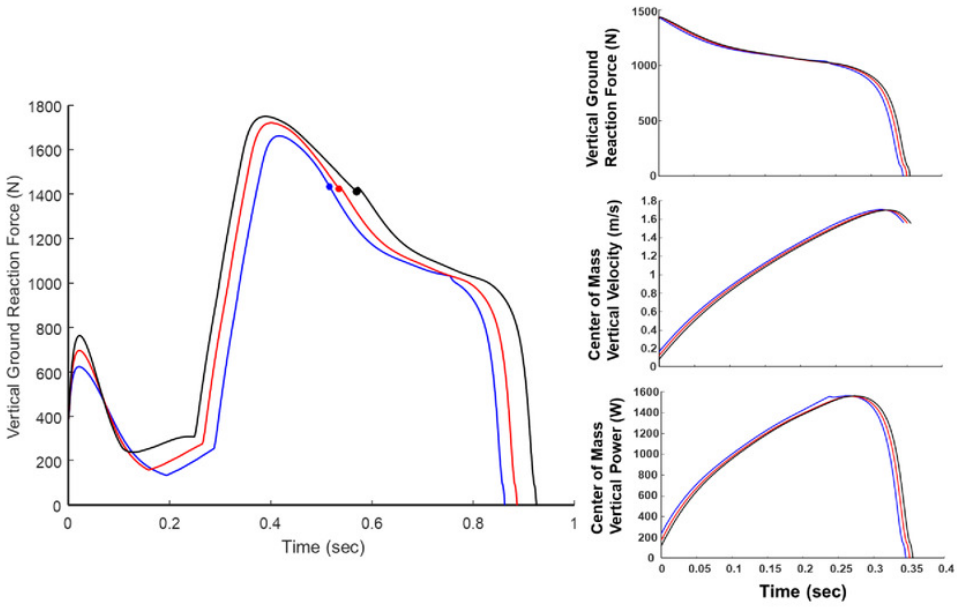
Vertical Ground Reaction Force (N)
Time (sec)
Vertical Ground Reaction Force (N)
Center of Mass Vertical Velocity (m/s)
Center of Mass Vertical Power (W)
Time (sec)

Figure 5

VAS activation, MTU force, tendon length, fiber length, and fiber velocity across normal, 15% AEL, and 30% AEL conditions.

The main graphs show the data for the entire jumping motion until take-off. The color-filled markers represent the time at the beginning of upward motion for each condition. The dashed blue lines represent the time when the tendon achieved its maximal length in the normal condition. The blue arrows indicate the change in length in the normal condition. Three different conditions were time-normalized from the beginning of upward motion to take-off (i.e. push-off phase), as shown in the smaller inset plots.

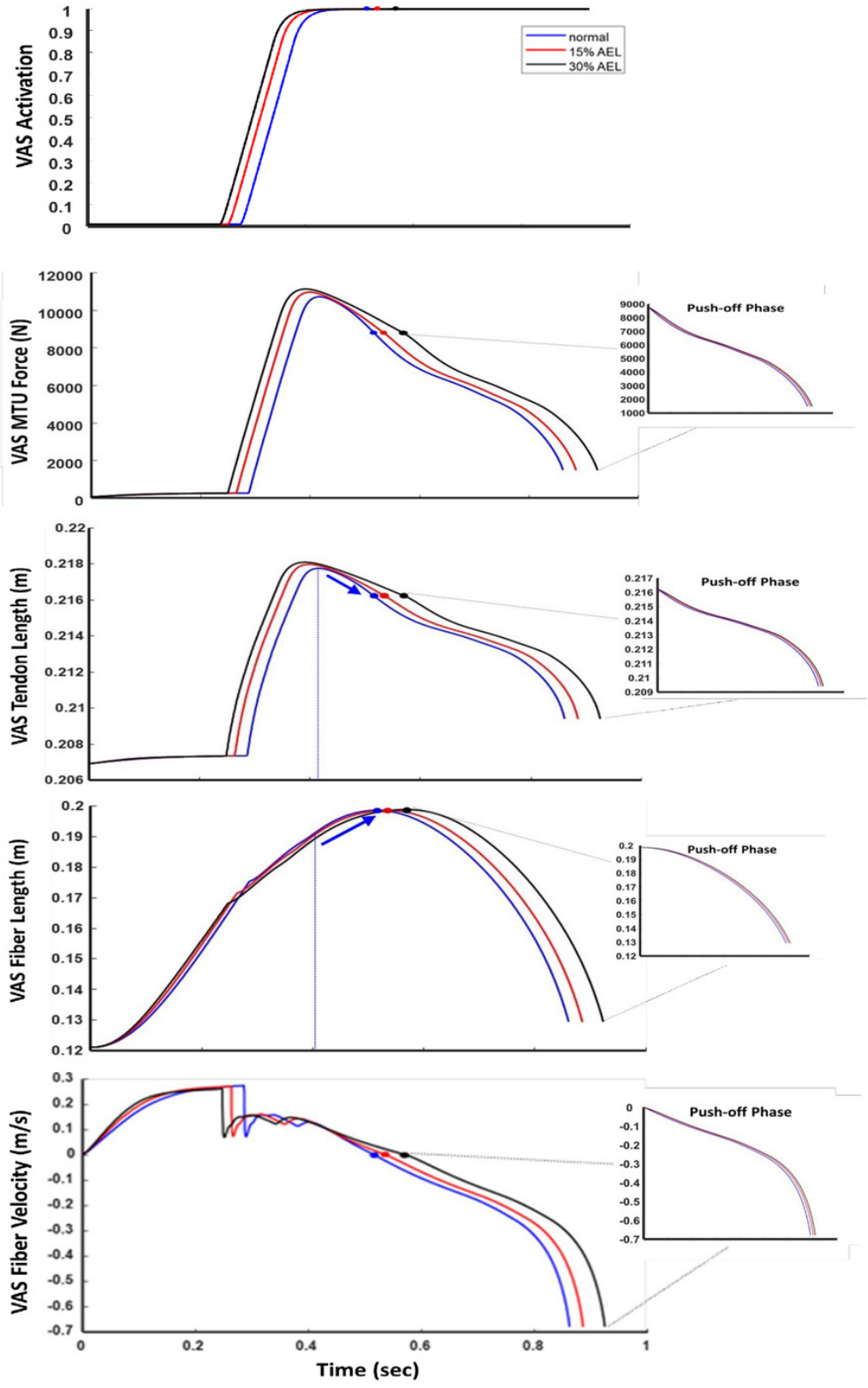
VAS Activation
normal
15% AEL
30% AEL
VAS MTU Force (N)
Push-off Phase
VAS Tendon Length (m)
Push-off Phase
VAS Fiber Length (m)
Push-off Phase
VAS Fiber Velocity (m/s)
Push-off Phase
Time (sec)